



Contents lists available at ScienceDirect

Neurobiology of Aging

journal homepage: www.elsevier.com/locate/neuaging

Reduced functional connectivity in early-stage drug-naïve Parkinson's disease: a resting-state fMRI study

ChunYan Luo^{a,1}, Wei Song^{a,1}, Qin Chen^a, ZhenZhen Zheng^a, Ke Chen^a, Bei Cao^a, Jing Yang^a, JianPeng Li^a, XiaoQi Huang^b, QiYong Gong^{b,**}, Hui-Fang Shang^{a,*}

^a Department of Neurology, West China Hospital, SiChuan University, Chengdu Sichuan, China

^b Huaxi MR Research Center, Department of Radiology, West China Hospital, SiChuan University, Chengdu Sichuan, China

ARTICLE INFO

Article history:

Received 26 April 2013

Received in revised form 15 July 2013

Accepted 16 August 2013

Keywords:

Parkinson's disease (PD)

Resting-state functional magnetic resonance imaging

Functional connectivity

Early stage

Drug naïve

Striatum

Mesolimbic regions

ABSTRACT

Although cardinal motor symptoms in Parkinson's disease (PD) are attributed to dysfunction of corticostriatal loops, early clinical nonmotor features are more likely to be associated with other pathologic mechanisms. We enrolled 52 early-stage drug-naïve PD patients and 52 age- and sex-matched healthy controls and used resting-state functional connectivity magnetic resonance imaging to evaluate alteration of the functional brain network in PD, focusing in particular on the functional connectivity of the striatum subregions. Relative to healthy controls, the PD patient group showed reduced functional connectivity in mesolimbic-striatal and corticostriatal loops. Although the decreased functional connectivity within cortical sensorimotor areas was only evident in the most affected putamen subregion, reduced functional connectivity with mesolimbic regions was prevalent throughout the striatum. No increased functional connectivity was found in this cohort. By studying a cohort of early-stage drug-naïve PD patients, we ruled out the potential confounding effect of prolonged antiparkinson medication use on the functional integration of neural networks. We demonstrate decreased functional integration across neural networks involving striatum, mesolimbic cortex, and sensorimotor regions in these patients and postulate that the prevalent disconnection in mesolimbic-striatal loops is associated with some early clinical nonmotor features in PD. This study offers additional insight into the early functional integration of neural networks in PD.

© 2013 Elsevier Inc. All rights reserved.

1. Introduction

Parkinson's disease (PD), the second most common neurodegenerative disease worldwide, is characterized by cardinal motor symptoms including tremor, rigidity, bradykinesia, and postural instability (Jankovic, 2008). Although PD is defined by its motor symptoms, many nonmotor symptoms (NMS) are also present (Chaudhuri and Schapira, 2009). Moreover, it has been widely accepted that some early NMS could indicate preclinical stages of PD before the onset of motor symptoms (Chaudhuri et al., 2011;

Nilsson et al., 2001; Ponsen et al., 2004; Postuma et al., 2006). For example, some researchers have observed that, apart from motor symptoms, depression is the initial symptom of PD (Jacob et al., 2010). Cardinal motor symptoms in PD are related to dysfunction of corticostriatal loops, which mainly result from progressive degeneration of dopaminergic neurons in the nigrostriatal pathway. However, early clinical nonmotor features are more likely to be associated with other pathologic mechanisms, such as impairment of nondopaminergic neuronal populations aside from the dopaminergic system (Dickson et al., 2009). In addition, post-mortem studies indicate pathologic processes may already occur in mesolimbic regions during the presymptomatic phase of PD (Braak et al., 2003), providing a pathologic basis for the occurrence of early nonmotor features in PD.

Substantial efforts have been made in the past decade to elucidate the neural basis of PD, with mounting evidence indicating that deficits in PD arise from system-level disturbances in the distributed neural network (Brooks and Pavese, 2011). Thus, by examining the human brain as an integrative network of functionally

* Corresponding author at: Department of Neurology, West China Hospital, Sichuan University, 610041, Chengdu, Sichuan, China. Tel.: +0086 18 980602127; fax: +0086 28 85423550.

** Alternate Corresponding author at: Huaxi MR Research Center, Department of Radiology, West China Hospital of Sichuan University, No. 37 Guo Xue Xiang Chengdu, 610041, China. Tel.: +0086 18 980601593; fax: +0086 28 85423503.

E-mail addresses: qiyonggong@hmrc.org.cn (QiYong Gong), hfshang2002@163.com (H.-F. Shang).

¹ These authors contributed equally to this work.

interacting brain regions, we can obtain new insights about large-scale neuronal communication in the brain. Resting-state functional magnetic resonance imaging (rfMRI) has increasingly been used to investigate the integration of neural networks at resting state. Low-frequency (0.01–0.08 Hz) fluctuations of the blood oxygen level–dependent (BOLD) signal observed during the resting state by rfMRI are considered to be physiologically meaningful and related to spontaneous neural activity (Cordes et al., 2001). Although task-based fMRI studies can assess disturbances in functional connectivity when patients perform a particular task, assessment of resting-state connectivity has a different and potentially broader significance because it requires minimal patient compliance, avoids potential performance confounds associated with cognitive activation paradigms, and is relatively easy to implement in clinical studies (Fox and Greicius, 2010).

A number of studies have applied this technique to investigate functional network characteristics of resting-state PD patients (Baudrexel et al., 2011; Hacker et al., 2012; Helmich et al., 2010; Kwak et al., 2010; Seibert et al., 2012; Skidmore et al., 2013; Wu et al., 2009, 2011), finding disrupted functional integration in corticostriatal loops (Hacker et al., 2012; Helmich et al., 2010; Kwak et al., 2010; Seibert et al., 2012). However, most of these experiments included PD patients who had been chronically exposed to antiparkinson medication, which has been reported to increase the functional connectivity of cognitive and motor pathways of the striatum in healthy adults (Kelly et al., 2009) and partially restore deficits in the functional brain network of patients with PD (Delaveau et al., 2010; Esposito et al., 2013; Palmer et al., 2009; Tessitore et al., 2002; Wu et al., 2009). It is possible that some abnormal functional integration of the brain network may be concealed by prolonged use of antiparkinson medication. Therefore, whether these abnormalities observed in previous studies reflect the primary pathophysiologic changes of PD or the functional reorganization due to prolonged dopaminergic treatment needs to be clarified.

According to Braak staging (Braak et al., 2003), the pathologic process of PD, occurring primarily in the brainstem, pursues an ascending course, reaching the neocortex in the final stage. Subcortical involvement prevails throughout the course of PD. However, corticostriatal loop dysfunction is the most common explanation for clinical deficits, and relatively little attention has been paid to the subcortical loops (Hacker et al., 2012). It remains unclear whether there are other circuits, such as subcortical loops, that function abnormally early in the natural course of PD when the “restoration” effect of antiparkinson medication is not in place. We hypothesized that alteration of functional integrity is not restricted to the corticostriatal loops and that more subcortical networks may be implicated. Compared with studies on chronic PD patients, study of drug-naïve PD patients may be critical to elucidate the core pathophysiology of this illness. This investigation is the first to use rfMRI to examine brain network integrity in a large cohort of early-stage, drug-naïve PD patients, together with the relationship between the Non-motor Symptoms Scale (NMSS) and alteration of functional connectivity.

2. Methods

2.1. Participant

Patients with PD were recruited from the movement disorders outpatient clinic of West China Hospital of Sichuan University from January 2010 to February 2012. All PD patients were diagnosed based on the UK PD Society Brain Bank Clinical Diagnostic Criteria (Hughes et al., 1992). Patients with secondary Parkinsonism and Parkinson-plus syndrome were excluded from this study. Demographic features and clinical data, including age, age of onset, sex, diagnostic delay, and disease duration, were collected using a standard

questionnaire by a movement disorder specialist during face-to-face interviews at the initial visit. For inclusion in the study, all the patients were required not to have been treated with antiparkinson medications at the initial visit (i.e., to be drug-naïve). The Unified PD Rating Scale (UPDRS) part III (Goetz et al., 2008; Hacker et al., 2012) was used to assess the motor disability, and Hoehn and Yahr (H&Y) stage (Hoehn and Yahr, 2001) was used to evaluate disease severity. Mini-Mental State Exam (MMSE) (Folstein et al., 1975;) was used to evaluate cognition. On the basis of previous studies using MMSE in Chinese (Katzman et al., 1988; Zhang et al., 1990), we used the following cutoff points to define abnormal MMSE in our patients: ≤ 17 for illiterate subjects, ≤ 20 for grade-school literate, and ≤ 23 for junior high school and higher education literate. The severity and frequency of NMS were assessed with the NMSS, which has been confirmed as an acceptable, reproducible, valid, and precise assessment instrument for NMS in the international populations (Chaudhuri et al., 2007). The NMSS is composed of 30 items grouped in 9 domains: cardiovascular, sleep/fatigue, mood/apathy, perceptual problems, attention/memory, gastrointestinal, urinary, sexual function, and miscellaneous. Each item is scored for severity (0 = none to 3 = severe) and frequency (1 = rarely to 4 = very frequent) and each item score was calculated by the product of both severity and frequency. A patient scoring ≥ 1 on 1 NMS item indicated that he or she presented with NMS. The maximum total score, which indicates the greatest NMS severity, is 360. Ratings were performed blinded to the MRI data set. Patients were excluded if they had (1) moderate-severe head tremor; (2) a history of head injury, stroke, or other neurologic disease; (3) disease duration > 4 years; (4) abnormal MMSE scores; and (5) any disorder that interfered with the assessment of the manifestation of PD.

Originally, 77 right-handed drug-naïve patients were recruited. These patients were followed up every 3 months at the movement disorder clinic. Finally, 52 PD patients were included in the study, whereas 25 patients were excluded for the following reasons: 3 patients for image distortion, 9 patients because of excessive head motion during the image acquisition; 2 patients were at H&Y stage 4 and had disease duration > 5 years; 11 patients had poor response to dopaminergic medication or emergence of nonparkinsonism symptoms during the follow-up period (range 12–36 months).

In addition, 52 right-handed healthy control subjects were recruited from the local area by poster advertisements. Healthy controls were assessed by a neurologist for their clinical condition. They were also assessed with the Structured Clinical Interview for the *Diagnostic and Statistical Manual of Mental Diseases* (4th edition), Nonpatient Edition, which was administered to each control participant by a psychiatrist trained to conduct this interview. Control subjects were excluded if they had (1) a history or present diagnosis of any *Diagnostic and Statistical Manual of Mental Diseases* Axis I diagnosis; (2) any neurologic illness, as assessed with clinical evaluations and medical records; or (3) organic brain defects on T1 or T2 images. All control participants were matched for age and sex to patients with PD. The local research ethics committee approved this study. All subjects gave written informed consent for participation.

2.2. MRI acquisition

MRI was performed on a 3.0-T magnetic resonance imaging system (Excite; GE, Milwaukee, WI, USA) by using an 8-channel phased-array head coil. High-resolution T1-weighted images were acquired via a volumetric 3-dimensional spoiled gradient recall sequence (repetition time = 8.5 milliseconds, echo time = 3.4 milliseconds, flip angle = 12° , slice thickness = 1 mm). Field of view ($240 \times 240 \text{ mm}^2$) was used with an acquisition matrix comprising 256 readings of 128-phase encoding steps that produced 156 contiguous coronal slices, with a slice thickness of 1.0 mm. The final matrix size of T1-weighted images was automatically interpolated

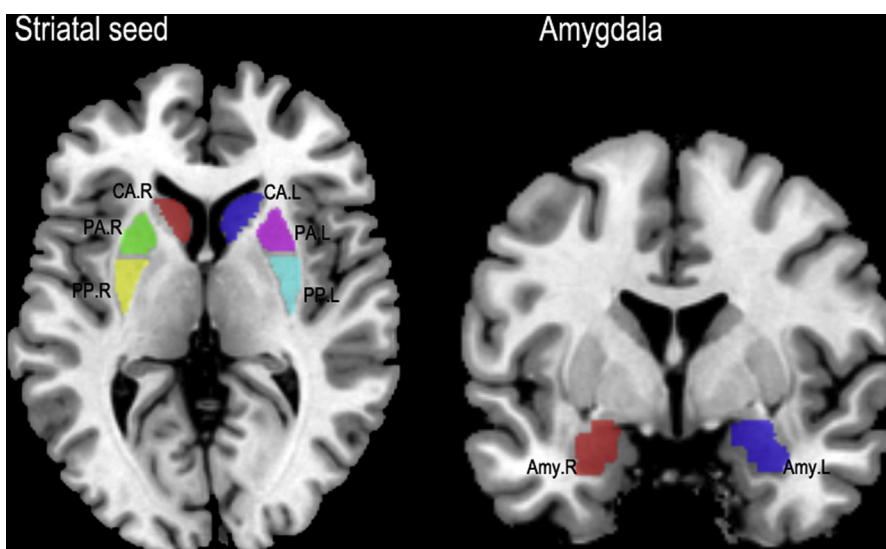


Fig. 1. Seed regions: anterior caudate, anterior putamen, posterior putamen, overlaid on Montreal Neurological Institute template. Abbreviations: CA, anterior caudate; L, left; PA, anterior putamen; PP, posterior putamen; R, right.

in-plane to 512×512 , which yielded an in-plane resolution of $0.47 \times 0.47 \text{ mm}^2$. Magnetic resonance images sensitive to changes in BOLD signal levels (repetition time = 2000 milliseconds, echo time = 30 milliseconds, flip angle = 90°) were obtained via a gradient-echo echo-planar imaging sequence (EPI). The slice thickness was 5 mm (no slice gap) with a matrix size of 64×64 and a field of view of $240 \times 240 \text{ mm}^2$, resulting in a voxel size of $3.75 \times 3.75 \times 5 \text{ mm}^3$. Each brain volume comprised 30 axial slices, and 1 functional run contained 200 image volumes. The fMRI scanning was performed in darkness, and the participants were explicitly instructed to relax, close their eyes, and not fall asleep (confirmed by subjects immediately after the experiment) during the rfMRI acquisition. Earplugs were used to reduce scanner noise, and head motion was minimized by stabilizing the head with cushions.

2.3. Preprocessing of fMRI data analysis

Functional image preprocessing and statistical analysis was carried out using the SPM8 (Wellcome Department of Imaging Neuroscience, London, UK; <http://www.fil.ion.ucl.ac.uk>). The first

10 volumes of functional images were discarded for the signal equilibrium and participants' adaptation to scanning noise. The remaining EPI images were then preprocessed using the following steps: slice timing, motion correction, spatial normalization to the standard Montreal Neurological Institute EPI template in SPM8 and resample to $3 \times 3 \times 3 \text{ mm}^3$, followed by spatial smoothing with 8-mm full-width at half-maximum Gaussian kernel. According to the record of head motions within each fMRI run, all participants had $<1.5 \text{ mm}$ maximum displacement in the x, y, or z plane and $<1.5^\circ$ of angular rotation about each axis. Analysis of head motion parameters in SPM8 did not reveal differences in motion correction parameters between the control group (mean translation: $0.26 \pm 0.13 \text{ mm}$, mean rotation: $0.27 \pm 0.15^\circ$) and the patient group (mean translation: $0.26 \pm 0.14 \text{ mm}$ for translation, $0.30 \pm 0.16^\circ$ for rotation) ($p > 0.05$).

2.4. Functional connectivity analysis

Functional connectivity was examined using a seed voxel correlation approach (Friston, 2011). On the basis of former

Table 1
Demographic and clinical characteristics for Parkinson's disease

	PD (n = 52)		Right onset (n = 31)		Left onset (n = 21)		Control (n = 52)	
	N	%	N	%	N	%	N	%
Handedness for writing (right)	52	100	31	100	21	100	52	100
Gender (female)	26	50	15	48.39	11	52.38	26	50
	Mean	SD	Mean	SD	Mean	SD	Mean	SD
Age (y)	52.28	9.41	51.20	9.23	53.87	9.55	51.17	9.23
Disease duration (mo)	23.31	17.67	25.89	20.13	19.49	12.76	—	—
Hoehn stage	1.85	0.63	1.86	0.67	1.83	0.58	—	—
UPDRS score								
Part I — mood/cognition	2.31	2.05	2.55	2.17	1.95	1.87	—	—
Part II — activities of daily living	8.02	4.38	7.97	3.78	8.10	5.23	—	—
Part III — motor examination	25.44	12.69	25.32	12.46	25.61	13.35	—	—
Part IV — complications of therapy	0	0	0	0	0	0	—	—
Total (sum of parts I–IV)	35.77	17.23	35.84	16.01	35.67	19.31	—	—
NMSS score	25.31	24.67	26.15	25.94	24.24	23.51	—	—
Mood Subscale Score	8.33	9.38	8.70	11.50	7.86	5.88	—	—
MMSE Score	27.15	2.89	27.13	2.90	27.19	2.94	—	—

Key: MMSE, Mini-Mental State Exam; NMSS, Non-Motor Symptoms Scale; UPDRS, Unified Parkinson's Disease Rating Scale.

neuroimaging findings, we selected left and right putamen and caudate as seeds. We defined the seed areas in the WFU (Wake Forest University) PickAtlas (<http://fmri.wfubmc.edu/software>) by overlapping the respective template from the automated anatomic labeling atlas (Lancaster et al., 2000; Tzourio-Mazoyer et al., 2002) Fig. 1. Furthermore, to account for the uneven amount of dopamine depletion in putamen in PD, which is most severe in the posterior putamen (Brück et al., 2006; Kish et al., 1988; Nurmi et al., 2001), we separated the putamen into a posterior and an anterior part. The border between these 2 regions was defined as the line passing through the anterior commissure (Helmich et al., 2010). A gap of 9 mm between the posterior and anterior subdivisions of the putamen in which voxels were excluded was left to avoid partial volume. The caudate nucleus was also subdivided into 2 parts according to the same anatomic rule of putamen subdivisions. Only the anterior caudate was included in the analysis; the posterior sector was excluded because of its small volumes and to prevent contamination with signals from the cerebrospinal fluid. Because the amygdala is a limbic region crucial for emotional processing and has been implicated in the neuropathology of early stage PD (Braak et al., 1994), we also selected amygdala as seeds. Eight regions of interest were resampled to $3 \times 3 \times 3 \text{ mm}^3$ standard space to enable extraction of time series from each subject's fMRI data.

Using REST (Song et al., 2011) (http://restfmri.net/forum/rest_v17), after bandpass filtering (0.01–0.08 Hz) (Cordes et al., 2001) and linear trend removal, the reference time series for each seed region was extracted by averaging the fMRI time series of all voxels within each region of interest. Correlation functional analyses were performed by computing temporal correlation between each seed reference and the rest of the brain in a voxel-wise manner. To remove the possible variances from time course of each voxel, 8 nuisance covariates were regressed, including the white matter signal, the cerebrospinal fluid signal, and 6 head-motion parameters. Then the correlation coefficients in each voxel were transformed to z value images using the Fisher r-to-z transformation to improve normality (Lowe et al., 1998). Thus, an entire brain z-value map was created for each subject.

The individual z-value map was entered into a random effect 2-sample *t* test to identify between-group differences in connectivity with the left and right posterior putamen, anterior putamen, anterior caudate, and amygdala. The significance threshold was set at $p < 0.001$ at voxel level and $p < 0.05$ corrected by family-wise error correction at cluster level. Age and gender were used as nuisance covariates in all statistical analysis. Dopamine depletion is uneven between bilateral putamen, which is more severe in the putamen contralateral to the side of onset. To avoid this potential confounding effect, we further divided the patients into left-onset and right-onset subgroups.

To characterize the abnormal functional connectivity between putamen and mesolimbic regions, we choose amygdala as representative of mesolimbic region and performed an additional post hoc region-wise functional connectivity analysis of amygdala-putamen circuit. Mean time series were extracted in left and right posterior putamen and amygdala by averaging the time series within seed region. The aforementioned procedures were used to remove possible variances from the mean time series of seeds. The resulting time series were correlated between seeds of each subject. A Fisher's *r*-to-*z* transformation was applied to normalize correlation coefficients. Two-sample 2-tailed *t* tests were performed between patients and controls. The statistical significance level was set to $p < 0.05$ (2 tailed). In addition, to explore whether this change correlated with NMS in PD patients, Pearson correlation analysis of functional connectivity between putamen and amygdala against the NMSS score and mood

subscale score was performed in patients with PD, and the significance was set at $p < 0.05$ (2-tailed).

2.5. Voxel-based morphometry analysis

Recent studies of fMRI have suggested that functional results could potentially be influenced by structural differences among groups (Oakes et al., 2007). To explore the possible effect, we performed a voxel-based morphometry (VBM) analysis for structural images. In this study, we used the diffeomorphic anatomic registration through an exponentiated lie algebra algorithm (DARTEL) (Ashburner, 2007) to improve the registration of the MRI images. DARTEL has been shown to be more sensitive than standard VBM methods (Klein et al., 2009). Before segmentation, we checked for scanner artifacts and gross anatomic abnormalities for each subject, and the image origin was set to the anterior commissure. MR images were then segmented into gray matter (GM), white matter, and cerebrospinal fluid using the unified segmentation model in SPM8 (Ashburner and Friston, 2005). In a next step, a GM template was generated through an iteratively nonlinear registration (DARTEL) (Ashburner, 2007). The GM

Table 2

Difference of functional connectivity between patients with Parkinson's disease and healthy comparison subjects

Seed area	Connected area	<i>t</i> value	MNI coordinates (x y z)	
Left anterior putamen Cluster 1 (size: 580; $p < 0.001$)	Rectus_R	5.65	24 15 -12	
	Olfactory_L	5.25	-21 15 -9	
	Putamen_R	5.16	27 -3 6	
Right anterior putamen Cluster 1 (size: 181; $p < 0.022$)	Frontal_inf_orb_R	4.89	24 15 -15	
	Amygdala_R	4.44	30 -3 -18	
	Putamen_L	4.70	-24 12 0	
	Hippocampus_L	4.47	-30 -12 -12	
Left posterior putamen Cluster 1 (size: 937; $p < 0.001$)	Putamen_R	5.28	30 -12 0	
	Insular_R	5.20	27 15 -15	
	Rectus_L	5.08	-24 12 -12	
	Postcentral_L	4.33	-42 -18 33	
	Pariatal_inf_L	4.09	-36 -39 33	
	Supramarginal_L	4.08	-48 -33 30	
	Temporal_mid_L	4.38	-54 -51 0	
	Cluster 3 (size: 199; $p = 0.016$)	Supramarginal_R	3.92	60 -33 48
	Cluster 4 (size: 177; $p = 0.025$)	Temporal_sup_R	3.77	57 -33 21
	Right posterior putamen Cluster 1 (size: 757, $p < 0.001$)	Putamen_L	5.24	-30 -6 0
Hippocampus_L		4.91	-30 -12 -12	
Postcentral_L		4.98	-45 -18 33	
Pariatal_inf_L		3.83	-36 -39 33	
Supeamarginal_L		3.67	-48 -33 33	
Temporal_mid_L		5.05	-54 -48 -3	
Cluster 3 (size: 156; $p = 0.035$)		Temporal_inf_L	3.58	-51 -45 -24
Right amygdala Cluster 1 (size: 424; $p < 0.001$)	Putamen_L	5.11	-24 0 6	
	Cluster 2 (size: 163; $p = 0.033$)	Putamen_R	4.55	27 9 -6

p values were corrected for multiple comparisons with family-wise error correction. Key: inf, inferior; mid, middle; MNI, Montreal Neurological Institute; orb, orbital; sup, superior.

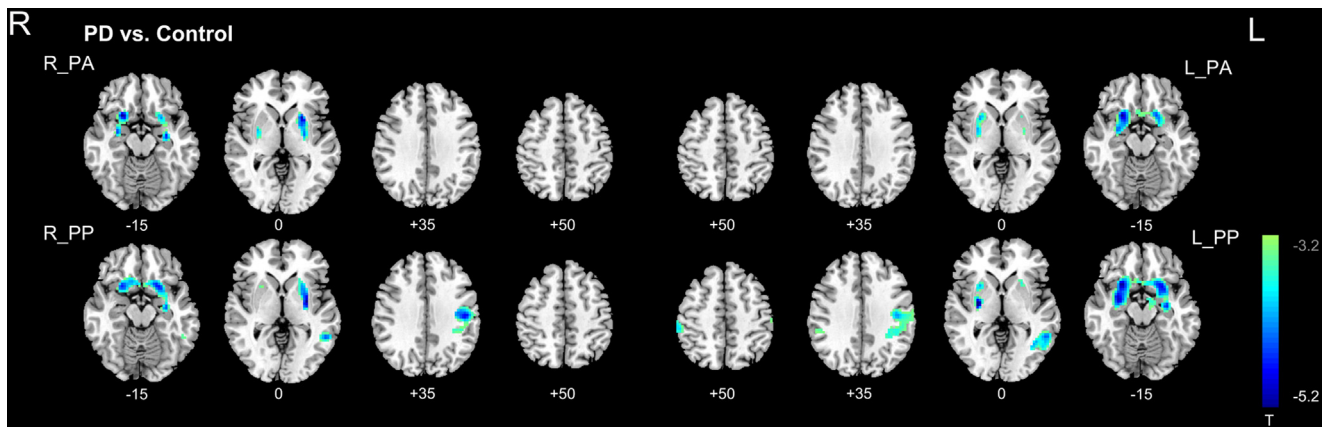


Fig. 2. Differences in the connectivity patterns of striatum in patients with Parkinson's disease. Functional connectivity of anterior putamen (PA) was significantly reduced in mesocortex and contralateral putamen. Functional connectivity of posterior putamen (PP) was significantly reduced in mesocortex, contralateral putamen, and sensorimotor cortex. The significance threshold was set at $p < 0.001$ at voxel level and $p < 0.05$ corrected by family-wise error correction at cluster level. Abbreviations: L, left; R, right.

template was normalized to Montreal Neurological Institute space, and the resulting deformations were applied to the GM images of each participant. Finally, spatially normalized images were modulated to ensure that the overall amount of each tissue class was not altered by the spatial normalization procedure and smoothed with an 8-mm full-width at half-maximum Gaussian kernel.

Voxel-based comparisons of GM volume were performed between groups using 2-sample t tests with total intracranial volume, age, and sex as covariates. The significance threshold was set at $p < 0.001$ at voxel level and $p < 0.05$ corrected by family-wise error correction at cluster level.

3. Results

3.1. Demographic and clinical characteristics

Age, sex, and handedness were not significantly different between the patients group and the healthy control group. Patients were at early stage of PD with mean disease duration of 23.31 ± 17.67 months (defined as the time since symptom onset). The average H&Y stage was 1.85 ± 0.63 (maximum stage = 3). The average motor score on the UPDRS was 25.44 ± 12.69 . Based on previous studies using the MMSE in Chinese (Katzman et al., 1988; Zhang et al., 1990), all patients' cognition was normal (MMSE: 27.15

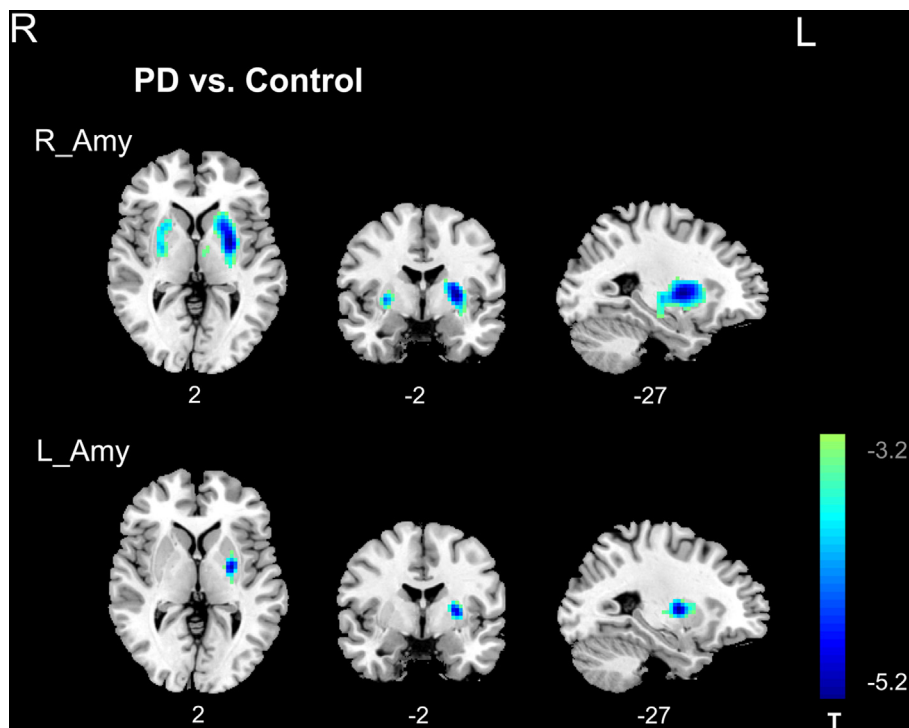


Fig. 3. Difference in the connectivity patterns of amygdala in patients with Parkinson's disease. Functional connectivity of right amygdala was reduced in putamen. Cluster in the T map of left amygdala did not surpass the threshold for multiple comparisons. The significance threshold was set at $p < 0.001$ at voxel level and $p < 0.05$ corrected by family-wise error correction at cluster level. Abbreviations: Amy, amygdala; L, left; R, right.

± 2.89). Four illiterate patients and 2 grade-school literate had MMSE scores <25 . UPDRS scores, H&Y stage, NMSS scores, and MMSE scores were not significantly different between right- and left-onset patient subgroups. The clinical data of PD patients are shown in [Table 1](#).

3.2. Between-group difference of functional connectivity analysis

Relative to the healthy control group, the PD patients showed significantly reduced connectivity within mesolimbic-striatal and corticostriatal loops ([Table 2](#), [Fig. 2](#)). Both anterior putamen and posterior putamen showed a decreased connectivity pattern with their contralateral putamen and mesolimbic regions, especially in amygdala, hippocampus, olfactory area, and posterior rectus, whereas the posterior putamen presented a more prominent decreased pattern extending to sensorimotor cortex. The caudate connectivity pattern was relatively spared. Functional connectivity analysis of the amygdala also showed coherent reduced connectivity pattern with the putamen ([Table 2](#), [Fig. 3](#)). To exclude group differences caused by the subgroup of patients with MMSE <25 , we reanalyzed the data and found similar striatal functional connectivity after excluding these 6 patients ([Supplemental Material](#)).

Results for comparison of PD subgroups versus healthy controls are shown in [Table 3](#) and [Fig. 4](#). The right-onset subgroup showed consistent decreased functional connectivity within mesolimbic-striatal and cortical-striatal loops, the extent of which followed the gradient of dopamine depletion in striatum. The decreased functional connectivity with sensorimotor cortex is only evident in the most affected posterior putamen. In the left-onset subgroup, only the right posterior putamen (the most affected striatum subregion) showed significantly reduced connectivity with left sensorimotor cortex and left putamen.

3.3. Region-wise functional connectivity analysis in the putamen-amygdala circuit

To characterize the abnormal functional connectivity between mesolimbic regions and the putamen, we choose amygdala as a representative of mesolimbic region. We assessed the correlation between the time course of the posterior putamen and that of amygdala and compared the magnitude of the correlation coefficients across groups. This revealed significantly decreased functional putamen-amygdala coupling in the whole PD group, as well as the right- and left-onset PD subgroups. Region-wise analysis is more sensitive than voxel-wise analysis in detecting abnormalities. The reduced functional putamen-amygdala coupling in the left-onset PD subgroup indicated a reduced trend of function connectivity in the mesolimbic-striatal loops of this subgroup. [Fig. 5](#) shows the means and SDs of z values in putamen-amygdala circuits.

We also searched for relationship between NMS (NMSS score and subscale score) and index of putamen-amygdala connectivity ([Fig. 6](#)). The functional coupling of right amygdala and left posterior putamen is significantly correlated with NMSS total score ($r = -0.44$, $p = 0.001$) and NMSS mood subscale score ($r = -0.45$, $p < 0.001$). The functional coupling of right amygdala and right posterior putamen is also significantly correlated with NMSS total score ($r = -0.40$, $p = 0.004$) and NMSS mood subscale score ($r = -0.36$, $p = 0.008$). No correlation was found between other NMSS subscale scores and functional connectivity in putamen-amygdala circuits.

3.4. VBM

VBM did not reveal significant differences between patients and healthy controls for GM volume, indicating that altered functional connectivity was not caused by anatomic changes.

Table 3

Difference of functional connectivity among subgroups of Parkinson's disease (PD) and healthy comparison subjects

Seed area	Connected area	t value	MNI coordinates (x y z)
A: right-onset PD < controls			
Left caudate			
Cluster 1 (size: 265; $p = 0.003$)	Putamen_R	4.47	15 12 -6
	Amygdala_R	3.66	27 0 -18
Left anterior putamen			
Cluster 1 (size: 196; $p = 0.009$)	Rectus_R	4.99	21 12 -15
	Putamen_R	4.13	24 0 9
	Amygdala_R	4.07	30 -3 -18
Cluster 2 (size: 177; $p = 0.014$)	Putamen_L	5.01	-24 12 -9
	Frontal_inf_orb_L	4.44	-18 15 -18
Right anterior putamen			
Cluster 1 (size: 337; $p = 0.001$)	Hippocampus_L	5.07	-30 -12 -12
	Olfactory_L	4.83	-27 9 -9
	Putamen_L	4.83	-27 6 3
Left posterior putamen			
Cluster 1 (size: 362; $p < 0.001$)	Rectus_L	5.13	-24 12 -12
	Hippocampus_L	4.80	-30 -9 -15
	Frontal_inf_tri_L	4.21	-33 30 9
Cluster 2 (size: 631; $p < 0.001$)	Amygdala_R	5.06	27 -3 -15
	Rectus_R	4.87	24 15 -12
	Putamen_R	4.69	24 12 0
Cluster 3 (size: 505; $p < 0.001$)	Supramarginal_R	4.95	60 -33 51
	Temporal_sup_R	4.15	57 -33 21
Cluster 4 (size: 654; $p < 0.001$)	Postcentral_L	4.72	-63 -6 30
	Precentral_L	4.54	-60 3 24
	Supramarginal_L	4.49	-51 -30 33
Cluster 5 (size: 303; $p = 0.001$)	Frontal_sup_orb_R	4.37	15 48 -24
	Cingulum_ant_L	4.31	-15 36 12
Right posterior putamen			
Cluster 1 (size: 272; $p = 0.002$)	Hippocampus_L	5.02	-30 -9 -12
	Putamen_L	4.66	-30 -9 0
	Rectus_L	4.21	-24 12 -12
Cluster 2 (size: 193; $p = 0.01$)	Frontal_sup_orb_R	4.48	12 18 -18
	Amygdala_R	4.19	30 -3 -18
B: left-onset PD < controls			
Right posterior putamen			
Cluster 1 (size: 254; $p = 0.003$)	Postcentral_L	4.71	-45 -18 39
Cluster 2 (size: 123; $p = 0.047$)	Putamen_L	4.41	-27 9 0

p value was corrected for multiple comparisons by family-wise error correction.

Key: ant, anterior; inf, inferior; L, left; MNI, Montreal Neurological Institute; orb, orbital; R, right; sup, superior; tri, triangular.

4. Discussion

By comparing a cohort of drug-naïve PD patients and healthy controls using rfMRI, we found decreased functional connectivity in mesolimbic-striatal and corticostriatal loops in the PD patients. No increased functional connectivity was found. The effect of PD on striatal function, in terms of reduced functional connectivity, was more prominent in the posterior putamen compared with the anterior putamen, in accordance with uneven dopamine depletion in the putamen in PD. Further functional connectivity analysis in the subgroups of right- and left-onset revealed similar results. Decreased functional connectivity within cortical sensorimotor areas was evident only in the most affected putamen subregion, whereas reduced functional connectivity within mesolimbic regions was

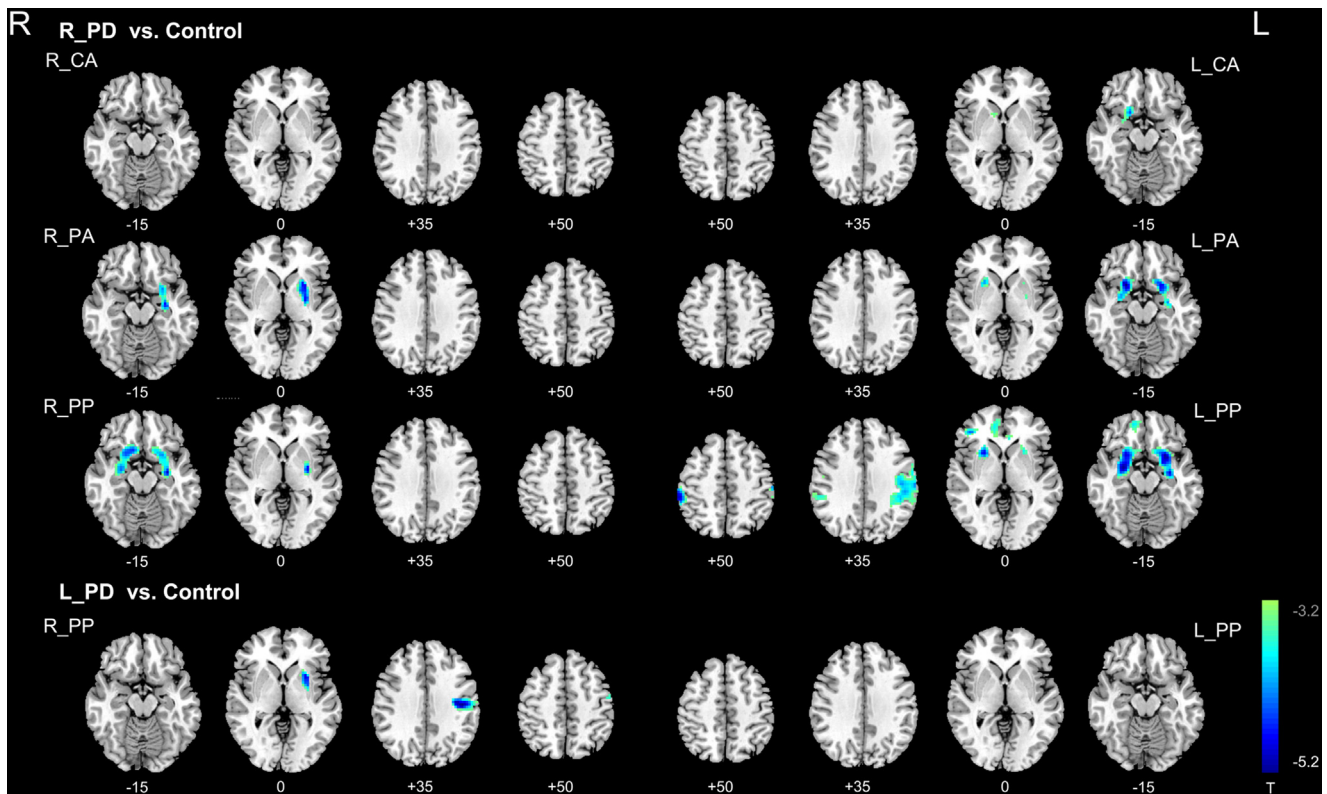


Fig. 4. Differences in the connectivity patterns of striatum in right-onset and left-onset Parkinson's disease subgroups. In the right-onset subgroup, functional connectivity of the left caudate, bilateral anterior putamen (AP), and right posterior putamen (PP) was significantly reduced in mesocortex and contralateral putamen, and functional connectivity left posterior putamen (most affected) was significantly reduced in mesocortex, contralateral putamen, sensorimotor cortex, and frontal cortex. In the left-onset subgroup, functional connectivity of the right posterior putamen (most affected) was significantly reduced in contralateral putamen and sensorimotor cortex. The significance threshold was set at $p < 0.001$ at voxel level and $p < 0.05$ corrected by family-wise error correction at cluster level. Abbreviations: CA, anterior caudate; L, left; R, right.

prevalent throughout the striatum, corresponding to Braak staging (Braak et al., 2003) in which the pathologic process of PD in the mesocortex has appeared in the presymptomatic stage, followed by involvement of the neocortex in later stages. Furthermore, the functional connectivity of amygdala-putamen was correlated with NMSS total score and NMSS mood subscore, indicating that functional deficiency in mesolimbic-striatal loops may be associated with underlying pathology of some nonmotor manifestations in PD.

Convergent evidence from functional brain imaging suggests that PD is associated with dysfunction in several functionally integrated pathways. More specifically, a loss of integrity among neural networks, especially in striatum circuitry, is thought to be at the root of the pathogenesis of PD. In our study, we demonstrated decreased functional connectivity of striatal circuits in early-stage drug-naïve patients with PD, which should reflect the primary changes in the natural disease course rather than secondary changes associated with prolonged antiparkinson medication.

Differences in striatal correlations with the cerebral cortex between PD patients and healthy controls were observed mainly between the posterior putamen and sensorimotor areas, whereas anterior putamen and caudate were relatively intact in terms of their functional correlations with the cortex. Further analysis in the subgroups of patients with right- or left-onset also revealed that the decreased functional connectivity with the cerebral cortex was only obvious in the posterior putamen. Evidence from postmortem and nuclear imaging studies have indicated that the posterior putamen suffers most from nigrostriatal dopamine depletion (Brück et al., 2006; Kish et al., 1988; Nurmi et al., 2001), and there is uneven amount of dopamine depletion in the bilateral putamen

(Marek et al., 1996; Morrish et al., 1995). The functional disconnection between the posterior putamen and sensorimotor areas observed in our study corresponds to those uneven pathologic changes in the striatum. The topography of the affected cortical regions is compatible with the impaired sensorimotor integration, which has been suggested to occur in PD (Almeida et al., 2005; Bäumer et al., 2007; Helmich et al., 2010; Konczak et al., 2009).

Two previous studies (Hacker et al., 2012; Helmich et al., 2010) using similar seed regions as ours in striatal subdivisions to explore the functional connectivity of the striatum also found loss of corticostriatal coupling in subregions of the putamen. Our results are broadly consistent with those findings. However, we observed comparatively less affected cortical connectivity with the putamen and failed to find increased functional connectivity in corticostriatal loops involving the anterior putamen, which was suggested to reflect compensatory changes in response to decreased functional connectivity between the sensorimotor cortex and posterior putamen (Helmich et al., 2010). We think the main contributor to this inconsistency is the patient inclusion. Patients in our cohort were in the early disease stage with mean disease duration of 2 ± 1.4 years, whereas the patients enrolled in Helmich et al.'s (2010) study had significantly longer disease duration (6.0 ± 0.6 years). Therefore, affected functional connectivity of the posterior putamen with the sensorimotor cortex in our patients was limited compared to that in Helmich et al.'s study; the response of the relatively spared anterior striatum might be too subtle to be detected by our study. In fact, we observed a slight trend of increased functional connectivity in corticostriatal loops involving the anterior striatum in the patient group (Supplementary Materials). As noted earlier, antiparkinson

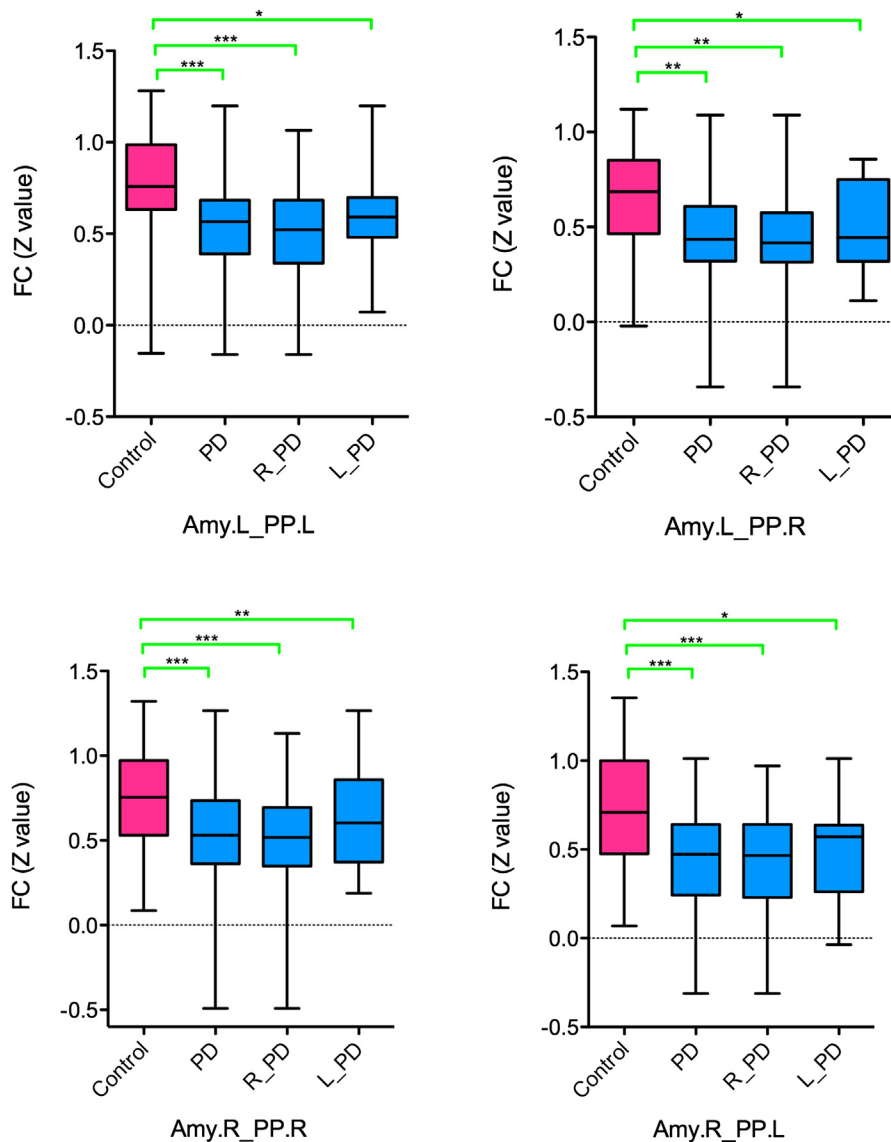


Fig. 5. Significant reduced functional connectivity between amygdala and posterior putamen in Parkinson's disease (PD) group and subgroups. Significant differences are indicated by asterisks: *** $p < 0.001$; ** $p < 0.01$; * $p < 0.05$. Abbreviations: Amy, amygdala; FC, functional connectivity; L, left; L_PD, left-onset PD; PP, posterior putamen; R, right; R_PD, right-onset PD.

medication can lead to functional reorganization of neural networks. It is likely that prolonged antiparkinson medication plays a role in this inconsistency. Differences in computational strategies may also play a role. The multiple regressions adopted by Helmich et al. have been suggested to be sensitive to differences between striatal subdivisions (e.g., remapping of corticostriatal connectivity) (Hacker et al., 2012).

Another inconsistency pertains to the involvement of subcortical networks. The study conducted by Hacker et al. (2012) additionally found that decreased striatal functional connectivity extended to the brainstem in PD patients, with relatively more severe motor disability (mean UPDRS III score in the off state: 39.1). In our study, we did not find obviously decreased striatal-extended brainstem functional connectivity. The brainstem remains a challenging part of the central nervous system from which to acquire functional MRI data, largely because of its small size, proximity to tissues producing magnetic susceptibility effects leading to image distortion, and the greater degree of noise in the BOLD MRI signal (Harvey et al., 2008). The image acquisition protocol we used was

not specifically designed for functional imaging of the brainstem. Further investigation is needed to determine the functional changes in the brainstem and its interaction with the striatum in PD.

We demonstrated decreased functional connectivity in mesolimbic-striatal loops in the resting state in early-stage drug-naïve PD patients. Differences in patient inclusion might contribute to this inconsistency. The mesocortex is the target of standard dopaminergic treatment (Jenner, 2002; Koller and Rueda, 1998), which may be more sensitive to the reorganization effects of prolonged medication. Our results avoid the confounding effects of prolonged antiparkinson medication and demonstrate decreased functional connectivity in mesolimbic-striatal loops in the natural course of PD. Nonetheless, longitudinal study is needed to elucidate the dynamic changes of the functional integration of subcortical networks.

PD is no longer considered a pure motor disorder but rather a systemic disease with variegated early NMS, such as impaired olfaction, emotional problems, and cognitive impairment (Ferrer, 2011; Gallagher and Schrag, 2012; Schwarz et al., 2011). Although

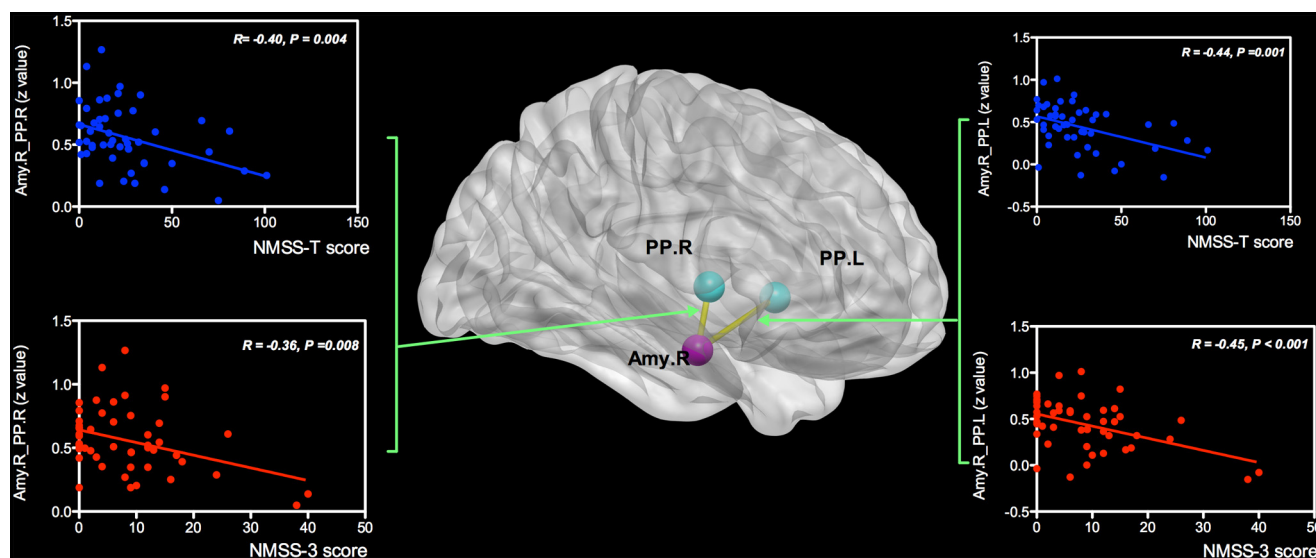


Fig. 6. Scatterplots showing a negative correlation between functional connectivity of the amygdala-putamen circuits and nonmotor scales ([NMSS]-T and NMSS-3) in Parkinson's disease patients. Abbreviations: Amy, amygdala; L, left; NMSS, Non-motor Symptoms Scale; NMSS-T, NMSS total score; NMSS-3, NMSS mood subscale score; PP, posterior putamen; R, right.

cardinal motor symptoms in PD are associated with dysfunction of corticostriatal loops, early clinical nonmotor features are more likely to be associated with other pathologic changes. In our study, apart from decreased functional connectivity in corticostriatal loops in PD, more prominent reduced functional connectivity was detected in mesolimbic-striatal loops, corresponding to the pre-symptomatic appearance of pathologic process in the mesocortex (Braak et al., 2003). The mesocortex regions are involved in a variety of functions, including emotion, motivation, cognition, olfaction, and sleep. Therefore, we speculate that abnormal integration of neural network involving the mesolimbic regions might be associated with NMS in PD.

In the past few years, neuroimaging research in humans (Barnes et al., 2010; Cohen et al., 2008; Di Martino et al., 2008; Draganski et al., 2008; Lehericy et al., 2004) has corroborated animal tracing studies (Haber, 2003; Parent, 1990) and shed further light on striatum circuitry and its relevance to clinical manifestations in PD. Consistent with estimates of striatal organization in the monkey (Alexander et al., 1986), these studies revealed broad topographic patterns that differentiate motor, cognitive, and affective zones of the striatum. Although functional subdivisions in the striatum have been demonstrated, the pattern of cortical coupling did not simply involve discrete regions of cortex. Rather, individual striatal regions were functionally coupled to distributed regions throughout the cerebellum (Barnes et al., 2010; Di Martino et al., 2008). Structural lesions (Braak et al., 2003) and/or changes in the neurotransmitter balance within the striatum and associated structures (Politis et al., 2010, 2012; Remy et al., 2005) could disrupt the process of integration of limbic input (Pavese et al., 2010), reflected by reduced functional connectivity in mesolimbic-striatal loops in our study. Taken together, these considerations fit with the idea that the decreased functional integrity in mesolimbic-striatal loops demonstrated by our study reflects pathologic changes of early nonmotor deficits in PD.

The amygdala, a limbic region crucial for emotional processing, has been implicated in the neuropathology of PD (Braak et al., 1994). Dysfunctions in PD such as impairment in facial expression recognition and mind reading (Levin et al., 1989) were reported in patients with focal amygdala damage (Stone et al., 2003). In addition, a postmortem study found that this structure contains Lewy

bodies in PD patients (Harding et al., 2002). Positron emission tomography and functional MRI studies (Ouchi et al., 1999; Tessitore et al., 2002) further confirmed the abnormal functions of amygdala in PD. In line with previous studies, functional connectivity analysis of amygdala revealed decreased functional coupling mainly with putamen in our study, which could be part of a larger picture of functional deficient between mesolimbic areas and putamen. Furthermore, negative correlations between functional connectivity of amygdala-putamen circuit and NMSS total score as well as NMSS mood subscale score suggest that functional disconnection of amygdala-putamen circuit might be related to mood disturbance in PD and also support the hypothesis that the reduced functional connectivity between mesolimbic areas and striatum is associated with NMS in early-stage PD. In our cohort, mood disturbance is one of the most often reported nonmotor problems, consistent with the high prevalence of emotional problem in the early stage of PD (Tan, 2011). Thus, it is plausible that both NMSS total score and mood subscale score show a negative correlation with the functional connectivity of amygdala-putamen circuit in the present study. However, future work is needed to verify this hypothesis with detailed evaluation of nonmotor manifestations and accounting for possible confounding factors.

Several study limitations should be considered when interpreting these results. First, the data are cross-sectional; whether these alterations of neural networks change dynamically after therapy remains to be established in the longitudinal studies. Second, in the subgroup of left-onset patients, a significant decreased connectivity pattern was only evident in the most affected putamen subregion, and we could not find reduced functional connectivity in the mesolimbic-striatal region at the current level of significance. This may be explained by the relatively stringent threshold of voxel-wise analysis and the small sample size of left-side onset. In the subsequent region-wise functional connectivity analysis, the left-side onset group demonstrated reduced functional connectivity in the amygdala-putamen circuit, indicating the reduced trend of function connectivity in mesolimbic-striatal loops. Third, although we have evaluated the nonmotor manifestations of patients using the NMSS, it is a cursory evaluation lacking specific neuropsychological assessment of particular aspects of PD, which hampers further interpretation of the results. Additional

investigations should focus on the relationship between functional network deficits and specific aspects of nonmotor manifestations.

In conclusion, our results confirm decreased functional connectivity in corticostriatal loops in a large cohort of drug-naïve PD patients. We also demonstrated reduced mesolimbic-striatal functional connectivity in this early-stage cohort, which might be associated with the underlying pathology of early nonmotor manifestations in PD. Although prolonged antiparkinson medication may lead to reorganization of functional neural networks through unknown mechanisms and confound our understanding of the primary pathologic process, our findings of prevalent reduced functional connectivity of neural networks in early-stage drug-naïve PD patients reflect the primary pathologic changes in the natural disease course.

Acknowledgements

This study was supported by the National Science Fund of China (grant 30973149) and the Science and Technology Bureau Fund of Sichuan Province (grant 2010SZ0069). The authors thank the patients for their participation in the study.

Appendix A. Supplementary data

Supplementary data associated with this article can be found, in the online version, at <http://dx.doi.org/10.1016/j.neurobiolaging.2013.08.018>.

Reference

- Alexander, G.E., DeLong, M.R., Strick, P.L., 1986. Parallel organization of functionally segregated circuits linking basal ganglia and cortex. *Annu. Rev. Neurosci.* 9, 357–381.
- Almeida, Q.J., Frank, J.S., Roy, E.A., Jenkins, M.E., Spaulding, S., Patla, A.E., Jog, M.S., 2005. An evaluation of sensorimotor integration during locomotion toward a target in Parkinson's disease. *Neuroscience* 134, 283–293.
- Ashburner, J., 2007. A fast diffeomorphic image registration algorithm. *Neuroimage* 38, 95–113.
- Ashburner, J., Friston, K.J., 2005. Unified segmentation. *Neuroimage* 26, 839–851.
- Barnes, K.A., Cohen, A.L., Power, J.D., Nelson, S.M., Dosenbach, Y.B.L., Miezin, F.M., Petersen, S.E., Schlaggar, B.L., 2010. Identifying basal ganglia divisions in individuals using resting-state functional connectivity MRI. *Front. Syst. Neurosci.* 4, 18.
- Baudrexel, S., Witte, T., Seifried, C., Wegner von, F., Beissner, F., Klein, J.C., Steinmetz, H., Deichmann, R., Roeper, J., Hilker, R., 2011. Resting state fMRI reveals increased subthalamic nucleus-motor cortex connectivity in Parkinson's disease. *Neuroimage* 55, 1728–1738.
- Bäumer, T., Pramstaller, P.P., Siebner, H.R., Schippling, S., Hagenah, J., Peller, M., Gerloff, C., Klein, C., Munchau, A., 2007. Sensorimotor integration is abnormal in asymptomatic Parkin mutation carriers: a TMS study. *Neurology* 69, 1976–1981.
- Braak, H., Braak, E., Yilmazer, D., Vos, R.A.I., Jansen, E.N.H., Bohl, J.R., Jellinger, K., 1994. Amygdala pathology in Parkinson's disease. *Acta Neuropathol.* 88, 493–500.
- Braak, H., Del Tredici, K., Rüb, U., de Vos, R.A.I., Jansen Steur, E.N.H., Braak, E., 2003. Staging of brain pathology related to sporadic Parkinson's disease. *Neurobiol. Aging* 24, 197–211.
- Brooks, D.J., Pavese, N., 2011. Imaging biomarkers in Parkinson's disease. *Prog. Neurobiol.* 95, 614–628.
- Brück, A., Aalto, S., Nurmi, E., Vahlberg, T., Bergman, J., Rinne, J.O., 2006. Striatal subregional 6-[18F]fluoro-L-dopa uptake in early Parkinson's disease: a two-year follow-up study. *Mov. Disord.* 21, 958–963.
- Chaudhuri, K.R., Martinez-Martin, P., Brown, R.G., Sethi, K., Stocchi, F., Odin, P., Ondo, W., Abe, K., MacPhee, G., MacMahon, D., Barone, P., Rabey, M., Forbes, A., Breen, K., Tluk, S., Naidu, Y., Olanow, W., Williams, A.J., Thomas, S., Rye, D., Tsuboi, Y., Hand, A., Schapira, A.H.V., 2007. The metric properties of a novel non-motor symptoms scale for Parkinson's disease: results from an international pilot study. *Mov. Disord.* 22, 1901–1911.
- Chaudhuri, K.R., Odin, P., Antonini, A., Martinez-Martin, P., 2011. Parkinson's disease: the non-motor issues. *Parkinsonism Relat. Disord.* 17, 717–723.
- Chaudhuri, K.R., Schapira, A.H., 2009. Non-motor symptoms of Parkinson's disease: dopaminergic pathophysiology and treatment. *Lancet Neurol.* 8, 464–474.
- Cohen, M.X., Lombardo, M.V., Blumenfeld, R.S., 2008. Covariance-based subdivision of the human striatum using T1-weighted MRI. *Eur. J. Neurosci.* 27, 1534–1546.
- Cordes, D., Haughton, V.M., Arfanakis, K., Carew, J.D., Turski, P.A., Moritz, C.H., Quigley, M.A., Meyerand, M.E., 2001. Frequencies contributing to functional connectivity in the cerebral cortex in “resting-state” data. *Am. J. Neuroradiol.* 22, 1326–1333.
- Delaveau, P., Salgado-Pineda, P., Fossati, P., Witjas, T., Azulay, J.-P., Blin, O., 2010. Dopaminergic modulation of the default mode network in Parkinson's disease. *Eur. Neuropsychopharmacol.* 20, 784–792.
- Di Martino, A., Scheres, A., Margulies, D.S., Kelly, A.M.C., Uddin, L.Q., Shehzad, Z., Biswal, B., Walters, J.R., Castellanos, F.X., Milham, M.P., 2008. Functional connectivity of human striatum: a resting state fMRI study. *Cereb. Cortex* 18, 2735–2747.
- Dickson, D.W., Fujishiro, H., Orr, C., DelleDonne, A., Josephs, K.A., Frigerio, R., Burnett, M., Parisi, J.E., Klos, K.J., Ahlskog, J.E., 2009. Neuropathology of non-motor features of Parkinson disease. *Parkinsonism Relat. Disord.* 15 (suppl 3), S1–S5.
- Draganski, B., Kherif, F., Klöppel, S., Cook, P.A., Alexander, D.C., Parker, G.J.M., Deichmann, R., Ashburner, J., Frackowiak, R.S.J., 2008. Evidence for segregated and integrative connectivity patterns in the human basal ganglia. *J. Neurosci.* 28, 7143–7152.
- Esposito, F., Tessitore, A., Giordano, A., De Micco, R., Paccone, A., Conforti, R., Pignataro, G., Annunziato, L., Tedeschi, G., 2013. Rhythm-specific modulation of the sensorimotor network in drug-naïve patients with Parkinson's disease by levodopa. *Brain* 136, 710–725.
- Ferrer, I., 2011. Neuropathology and neurochemistry of nonmotor symptoms in Parkinson's disease. *Parkinsons Dis.* 2011, 1–13.
- Folstein, M.F., Folstein, S.E., McHugh, P.R., 1975. “Mini-Mental State.” A practical method for grading the cognitive state of patients for the clinician. *J. Psychiatr. Res.* 12, 189–198.
- Fox, M.D., Greicius, M., 2010. Clinical applications of resting state functional connectivity. *Front. Syst. Neurosci.* 4, 19.
- Friston, K.J., 2011. Functional and effective connectivity: a review. *Brain Connect.* 1, 13–36.
- Gallagher, D.A., Schrag, A., 2012. Psychosis, apathy, depression and anxiety in Parkinson's disease. *Neurobiol. Dis.* 46, 581–589.
- Goetz, C.G., Tilley, B.C., Shaftman, S.R., Stebbins, G.T., Fahn, S., Martinez-Martin, P., Poewe, W., Sampaio, C., Stern, M.B., Dodel, R., Dubois, B., Holloway, R., Jankovic, J., Kulisevsky, J., Lang, A.E., Lees, A., Leurgans, S., LeWitt, P.A., Nyenhuis, D., Olanow, C.W., Rascol, O., Schrag, A., Teresi, J.A., van Hilten, J.J., LaPelle, N., 2008. Movement Disorder Society-sponsored revision of the Unified Parkinson's Disease Rating Scale (MDS-UPDRS): scale presentation and clinimetric testing results. *Mov. Disord.* 23, 2129–2170.
- Haber, S.N., 2003. The primate basal ganglia: parallel and integrative networks. *J. Chem. Neuroanat.* 26, 317–330.
- Hacker, C.D., Perlmutter, J.S., Criswell, S.R., Ances, B.M., Snyder, A.Z., 2012. Resting state functional connectivity of the striatum in Parkinson's disease. *Brain* 135, 3699–3711.
- Harding, A.J., Stimson, E., Henderson, J.M., Halliday, G.M., 2002. Clinical correlates of selective pathology in the amygdala of patients with Parkinson's disease. *Brain* 125, 2431–2445.
- Harvey, A.K., Pattinson, K.T.S., Brooks, J.C.W., Mayhew, S.D., Jenkinson, M., Wise, R.G., 2008. Brainstem functional magnetic resonance imaging: disentangling signal from physiological noise. *J. Magn. Reson. Imaging* 28, 1337–1344.
- Helmich, R.C., Derix, L.C., Bakker, M., Scheeringa, R., Bloem, B.R., Toni, I., 2010. Spatial remapping of cortico-striatal connectivity in Parkinson's disease. *Cereb. Cortex* 20, 1175–1186.
- Hoehn, M.M., Yahr, M.D., 2001. Parkinsonism: onset, progression, and mortality. *1967. Neurology* 57, S11–S26.
- Hughes, A.J., Daniel, S.E., Kilford, L., Lees, A.J., 1992. Accuracy of clinical diagnosis of idiopathic Parkinson's disease: a clinico-pathological study of 100 cases. *J. Neurol. Neurosurg. Psychiatry* 55, 181–184.
- Jacob, E.L., Gatto, N.M., Thompson, A., Bordelon, Y., Ritz, B., 2010. Occurrence of depression and anxiety prior to Parkinson's disease. *Parkinsonism Relat. Disord.* 16, 576–581.
- Jankovic, J., 2008. Parkinson's disease: clinical features and diagnosis. *J. Neurol. Neurosurg. Psychiatry* 79, 368–376.
- Jenner, P., 2002. Pharmacology of dopamine agonists in the treatment of Parkinson's disease. *Neurology* 58, S1–S8.
- Katzman, R., Zhang, M.Y., Ouang-Ya-Qu, Wang, Z.Y., Liu, W.T., Yu, E., Wong, S.C., Salmon, D.P., Grant, I., 1988. A Chinese version of the Mini-Mental State Examination; impact of illiteracy in a Shanghai dementia survey. *J. Clin. Epidemiol.* 41, 971–978.
- Kelly, C., de Zubicar, G., Di Martino, A., Copland, D.A., Reiss, P.T., Klein, D.F., Castellanos, F.X., Milham, M.P., McMahon, K., 2009. L-dopa modulates functional connectivity in striatal cognitive and motor networks: a double-blind placebo-controlled study. *J. Neurosci.* 29, 7364–7378.
- Kish, S.J., Shannak, K., Hornykiewicz, O., 1988. Uneven pattern of dopamine loss in the striatum of patients with idiopathic Parkinson's disease. Pathophysiologic and clinical implications. *N. Engl. J. Med.* 318, 876–880.
- Klein, A., Andersson, J., Ardekani, B.A., Ashburner, J., Avants, B., Chiang, M.C., Christensen, G.E., Collins, D.L., Gee, J., Hellier, P., Song, J.H., Jenkinson, M., Lepage, C., Rueckert, D., Thompson, P., Vercauteren, T., Woods, R.P., Mann, J.J., Parsey, R.V., 2009. Evaluation of 14 nonlinear deformation algorithms applied to human brain MRI registration. *Neuroimage* 46, 786–802.
- Koller, W.C., Rueda, M.G., 1998. Mechanism of action of dopaminergic agents in Parkinson's disease. *Neurology* 50, S11–S14.
- Konczak, J., Corcos, D.M., Horak, F., Poizner, H., Shapiro, M., Tuite, P., Volkman, J., Maschke, M., 2009. Proprioception and motor control in Parkinson's disease. *J. Mot. Behav.* 41, 543–552.

- Kwak, Y., Peltier, S., Bohnen, N.I., Müller, M.L., Dayalu, P., Seidler, R.D., 2010. Altered resting state cortico-striatal connectivity in mild to moderate stage Parkinson's disease. *Front. Syst. Neurosci.* 4, 143.
- Lancaster, J.L., Woldorff, M.G., Parsons, L.M., Liotti, M., Freitas, C.S., Rainey, L., Kochunov, P.V., Nickerson, D., Mikiten, S.A., Fox, P.T., 2000. Automated Talairach atlas labels for functional brain mapping. *Hum. Brain Mapp.* 10, 120–131.
- Lehéricy, S., Ducros, M., Van de Moortele, P.-F., Francois, C., Thivard, L., Poupon, C., Swindale, N., Ugurbil, K., Kim, D.-S., 2004. Diffusion tensor fiber tracking shows distinct corticostriatal circuits in humans. *Ann. Neurol.* 55, 522–529.
- Levin, B.E., Llabre, M.M., Weiner, W.J., 1989. Cognitive impairments associated with early Parkinson's disease. *Neurology* 39, 557–561.
- Lowe, M.J., Mock, B.J., Sorenson, J.A., 1998. Functional connectivity in single and multislice echoplanar imaging using resting-state fluctuations. *Neuroimage* 7, 119–132.
- Marek, K.L., Seibyl, J.P., Zoghbi, S.S., Zea-Ponce, Y., Baldwin, R.M., Fussell, B., Charney, D.S., van Dyck, C., Hoffer, P.B., Innis, R.B., 1996. [sup 123 I] beta-CIT/SPECT imaging demonstrates bilateral loss of dopamine transporters in hemi-Parkinson's disease. *Neurology* 46, 231–237.
- Morrish, P.K., Sawle, G.V., Brooks, D.J., 1995. Clinical and [18F] dopa PET findings in early Parkinson's disease. *J. Neurol. Neurosurg. Psychiatry* 59, 597–600.
- Nilsson, F.M., Kessing, L.V., Bolwig, T.G., 2001. Increased risk of developing Parkinson's disease for patients with major affective disorder: a register study. *Acta Psychiatr. Scand.* 104, 380–386.
- Nurmi, E., Ruottinen, H.M., Bergman, J., Haaparanta, M., Solin, O., Sonninen, P., Rinne, J.O., 2001. Rate of progression in Parkinson's disease: a 6-[18F]fluoro-L-dopa PET study. *Mov. Disord.* 16, 608–615.
- Oakes, T.R., Fox, A.S., Johnstone, T., Chung, M.K., Kalin, N., Davidson, R.J., 2007. Integrating VBM into the General Linear Model with voxelwise anatomical covariates. *Neuroimage* 34, 500–508.
- Ouchi, Y., Yoshikawa, E., Okada, H., Futatsubashi, M., Sekine, Y., Iyo, M., Sakamoto, M., 1999. Alterations in binding site density of dopamine transporter in the striatum, orbitofrontal cortex, and amygdala in early Parkinson's disease: compartment analysis for beta-CFT binding with positron emission tomography. *Ann. Neurol.* 45, 601–610.
- Palmer, S.J., Eigenraam, L., Hoque, T., McCaig, R.G., Troiano, A., McKeown, M.J., 2009. Levodopa-sensitive, dynamic changes in effective connectivity during simultaneous movements in Parkinson's disease. *Neuroscience* 158, 693–704.
- Parent, A., 1990. Extrinsic connections of the basal ganglia. *Trends Neurosci.* 13, 254–258.
- Pavese, N., Metta, V., Bose, S.K., Chaudhuri, K.R., Brooks, D.J., 2010. Fatigue in Parkinson's disease is linked to striatal and limbic serotonergic dysfunction. *Brain* 133, 3434–3443.
- Politis, M., Wu, K., Loane, C., Quinn, N.P., Brooks, D.J., Oertel, W.H., Bjorklund, A., Lindvall, O., Piccini, P., 2012. Serotonin neuron loss and nonmotor symptoms continue in Parkinson's patients treated with dopamine grafts. *Sci. Transl. Med.* 4, 128ra41.
- Politis, M., Wu, K., Loane, C., Turkheimer, F.E., Molloy, S., Brooks, D.J., Piccini, P., 2010. Depressive symptoms in PD correlate with higher 5-HTT binding in raphe and limbic structures. *Neurology* 75, 1920–1927.
- Ponsen, M.M., Stoffers, D., Booij, J., van Eck-Smit, B.L.F., Wolters, E.C., Berendse, H.W., 2004. Idiopathic hyposmia as a preclinical sign of Parkinson's disease. *Ann. Neurol.* 56, 173–181.
- Postuma, R.B., Lang, A.E., Massicotte-Marquez, J., Montplaisir, J., 2006. Potential early markers of Parkinson disease in idiopathic REM sleep behavior disorder. *Neurology* 66, 845–851.
- Remy, P., Doder, M., Lees, A., Turjanski, N., Brooks, D., 2005. Depression in Parkinson's disease: loss of dopamine and noradrenaline innervation in the limbic system. *Brain* 128, 1314–1322.
- Schwarz, J., Odin, P., Buhmann, C., Csoti, I., Jost, W., Wullner, U., Storch, A., 2011. Depression in Parkinson's disease. *J. Neurol.* 258, 336–338.
- Seibert, T.M., Murphy, E.A., Kaestner, E.J., Brewer, J.B., 2012. Interregional correlations in Parkinson disease and Parkinson-related dementia with resting functional MR imaging. *Radiology* 263, 226–234.
- Skidmore, F.M., Yang, M., Baxter, L., Deneen von, K.M., Collingwood, J., He, G., White, K., Korenkevych, D., Savenkov, A., Heilman, K.M., Gold, M., Liu, Y., 2013. Reliability analysis of the resting state can sensitively and specifically identify the presence of Parkinson disease. *Neuroimage* 75, 249–261.
- Song, X.W., Dong, Z.Y., Long, X.Y., Li, S.F., Zuo, X.N., Zhu, C.Z., He, Y., Yan, C.G., Zang, Y.F., 2011. REST: a toolkit for resting-state functional magnetic resonance imaging data processing. *PLoS One* 6, e25031.
- Stone, V.E., Baron-Cohen, S., Calder, A., Keane, J., Young, A., 2003. Acquired theory of mind impairments in individuals with bilateral amygdala lesions. *Neuropsychologia* 41, 209–220.
- Tan, L.C.S., 2011. Mood disorders in Parkinson's disease. *Parkinsonism Relat. Disord.* 18, S74–S76.
- Tessitore, A., Hariri, A.R., Fera, F., Smith, W.G., Chase, T.N., Hyde, T.M., Weinberger, D.R., Mattay, V.S., 2002. Dopamine modulates the response of the human amygdala: a study in Parkinson's disease. *J. Neurosci.* 22, 9099–9103.
- Tzourio-Mazoyer, N., Landeau, B., Papathanassiou, D., Crivello, F., Etard, O., Delcroix, N., Mazoyer, B., Joliot, M., 2002. Automated anatomical labeling of activations in SPM using a macroscopic anatomical parcellation of the MNI MRI single-subject brain. *Neuroimage* 15, 273–289.
- Wu, T., Long, X., Wang, L., Hallett, M., Zang, Y., Li, K., Chan, P., 2011. Functional connectivity of cortical motor areas in the resting state in Parkinson's disease. *Hum. Brain Mapp.* 32, 1443–1457.
- Wu, T., Long, X., Zang, Y., Wang, L., Hallett, M., Li, K., Chan, P., 2009. Regional homogeneity changes in patients with Parkinson's disease. *Hum. Brain Mapp.* 30, 1502–1510.
- Zhang, M.Y., Katzman, R., Salmon, D., Jin, H., Cai, G.J., Wang, Z.Y., Qu, G.Y., Grant, I., Yu, E., Levy, P., 1990. The prevalence of dementia and Alzheimer's disease in Shanghai, China: impact of age, gender, and education. *Ann. Neurol.* 27, 428–437.